State-selective differential cross sections for double-electron capture in 0.25–0.75-MeV He^{2+}-He collisions

R. Dörner,[1,*] V. Mergel,[1] L. Spielberger,[1] O. Jagutzki,[1] J. Ullrich,[2] and H. Schmidt-Böcking[1]
[1]*Institut für Kernphysik, Universität Frankfurt, August Euler Straße 6, D60486 Frankfurt, Germany*
[2]*GSI, D64291 Darmstadt, Germany*
(Received 19 June 1997)

For 0.25–0.75-MeV He^{2+} on He collisions we have measured total state selective double capture cross sections and cross sections differential in projectile scattering angle. For 0.25 MeV we present also state-selective scattering-angle-dependent double-capture cross sections. The projectile energy loss (the final electronic state) as well as the transverse momentum transfer (i.e., the projectile scattering angle) have been obtained by measuring the momentum vector of the recoil ion using cold target recoil ion momenum spectroscopy. The resonant transfer to the ground state is found to be by far the dominant double-capture channel. Capture to nonautoionizing excited states is smaller by about a factor of 7, and results in larger scattering angles than the ground-state double capture. [S1050-2947(98)06801-2]

PACS number(s): 34.50.−s, 34.70.+e

I. INTRODUCTION

Double-electron capture is a particularly interesting case of a two-electron process. For the He^{2+}-He system the forces of the nuclei on the electrons is of comparable strength to the electron-electron interaction. Thus the details of the transfer of the two electrons from a bound state of the target to a bound state of the projectile are sensitive to the static electron-electron correlation in the initial and final state, as well as to the dynamic correlation during the collision. For this capture reaction the resonant channel is predicted to be the dominant one for swift He^{2+}-He collisions [1]. However, up to now there was no experimental technique available which allowed one to isolate this reaction channel experimentally. Since the ejectile is neutral it cannot be analyzed by conventional energy-gain spectroscopy. So the few state selective cross sections which have been reported for the He^{2+}-He system were obtained exploiting the $(4\rightarrow 3)$ line emission [2] or the Auger decay of doubly excited states [3], and were therefore unable to detect the ground state. In this work we have used cold target recoil ion momentum spectroscopy (COLTRIMS) (for a recent review, see Ref. [4]). It offers a unique indirect but extremely precise way to determine the final state of the projectile, even for a neutral ground state, together with its scattering angle. Instead of the energy loss and the scattering angle of the projectile itself, we measured simultaneously the longitudinal (i.e., in the beam direction) ($p_{\parallel_{\mathrm{rec}}}$) and transverse momentum ($p_{\perp_{\mathrm{rec}}}$) recoiling of the He^{2+} ion. Since there are only two particles in the final state, the momentum change of the projectile must be exactly compensated for by the momentum change of the recoil ion. Thus analyzing the longitudinal momentum of the recoil ion is equivalent to translational spectroscopy of the projectile, and the determination of the recoil ion transverse momentum is equivalent to a scattering-angle measurement of the projectile [4–11].

For a capture reaction where n_e electrons are transferred to bound projectile states, and no electron is emitted into the continuum, $p_{\parallel\mathrm{rec}}$ is given from energy and momentum conservation to be

$$p_{\parallel\mathrm{rec}}=\frac{\Delta E}{v_{\mathrm{pro}}}-\frac{n_e\times v_{\mathrm{pro}}}{2}. \tag{1}$$

v_{pro} denotes the projectile velocity, and ΔE is the energy difference between the final and the initial state (endogenic reactions result in positive ΔE). Atomic units (a.u.) are used throughout this paper. For the perpendicular momentum one obtains

$$p_{\perp\mathrm{rec}}=p_{\mathrm{pro}}\tan\vartheta_{\mathrm{pro}}. \tag{2}$$

p_{pro} is the initial (longitudinal) momentum of the projectile, and ϑ_{pro} the projectile scattering angle.

Compared to conventional projectile energy-gain spectroscopy and projectile scattering-angle measurements, COLTRIMS has two main advantages. It is also applicable for neutral emerging projectiles, and allows one to achieve an excellent resolution even at high impact energies and poor momentum preparation of the incoming beam. The traditional projectile energy-gain technique as well as projectile deflection measurements are limited by the accuracy reachable in defining the huge initial projectile momentum to about $\Delta E/E=10^{-4}$. In contrast, the quality of the beam enters only in second order into the determination of the momentum transfer in a recoil ion momentum measurement. Therefore in the present experiment we reached a resolution of $\Delta E/E=\pm 1.5^{-5}$ at 0.75-MeV impact energy, and a scattering-angle resolution of better than $\pm 10^{-5}$ rad.

Over the last years more and more refined theoretical approaches on double-electron capture for the He^{2+} on He system became available. At low impact energies, coupled-channel calculations mostly using molecular-orbital basis sets and time-dependent Hartree-Fock calculations, have been performed [12–19]. At higher energies various forms of the independent-particle model [20] have been frequently ap-

*Electronic address: doerner@ikf.uni-frankfurt.de

plied. To calculate the single-particle transition amplitudes, some authors completely neglected correlations by exploiting uncorrelated wave functions [21]. Others included correlation in the initial and final states (so-called static correlation) by employing different types of correlated wave functions [22]. Various pertubative approaches like the continuum distorted wave (CDW) and the CDW–eikonal initial state (EIS) approximation [23–25,22,26] or the coupled-channel approach [21,27] have been used. Also, Olson and co-workers exploited the classical trajectory Monte Carlo model to obtain single-particle transition probabilities [28,29]. Crothers and McCaroll developed the independent-event model, in which double capture is still assumed to be a two-step process, but different wave functions are used to calculate the first- and second-step transition amplitudes [30–32] (see also Ref. [33]). Recently some approaches have been formulated which even preserve the four-body nature of the double-electron capture [1,34–40]. and successfully circumvent the restrictions of the independent-electron model.

From the experimental side the situation is significantly worse. A comprehensive set of data is available only for total double-capture cross sections [41–44]. However total cross sections allow only a very crude test of elaborate theories. Differential and state-selective cross sections are needed for a detailed comparison with the different theoretical approaches. Many of the dynamic mechanisms responsible for the capture process will only show up in differential cross sections. For single capture in the high-energy regime the Thomas mechanism is a prominent example of this. For double capture even three different Thomas-type mechanisms have been predicted to become visible in the differential cross section [39,23]. For low impact energies the interference structures resulting from transitions between molecular orbitals on the incoming and outgoing trajectory demonstrate the power of differential cross sections for illuminating the mechanisms behind the capture process [8,45].

So far, for He^{2+} on He no state-selective and scattering-angle-dependent cross sections are available for double capture. At energies below 10 keV, in the regime of molecular-orbital calculations, Keever and Everhart [45] reported differential cross sections which sum over all final states. The same has been measured at higher energies (1.5 MeV) [44]. This latter data set, the only one at higher energies, has been widely used for comparison with various calculations. However, in most cases it was not sufficient to draw final conclusions about the validity of the different theoretical approaches. The main problem was the resolution in the scattering-angle measurement.

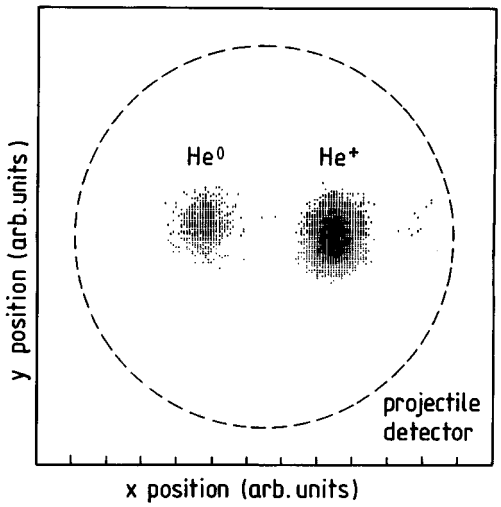

FIG. 1. Position distribution of the He^+ (right) and He (left) ejectiles on a two-dimensional position-sensitive channel plate detector. The charge states have been separated by electrostatic deflectors.

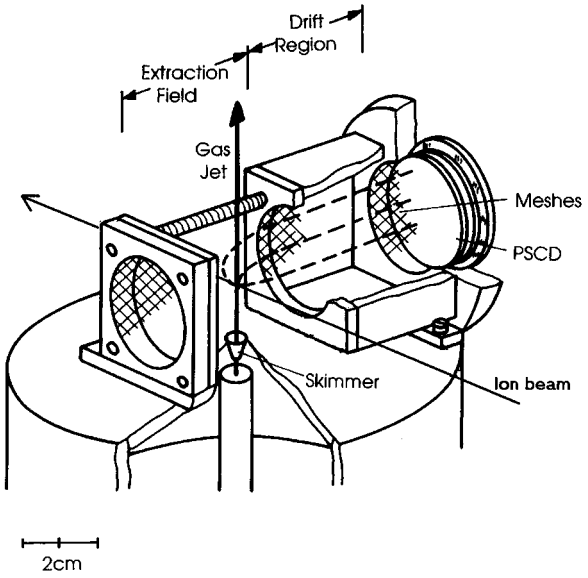

FIG. 2. Cold target recoil ion momentum spectrometer as used for this experiment. The precooled supersonic gas jet produces a localized and internally cold gas target. The extraction field is 0.33 V/cm. The ions are detected by a two-dimensional position sensitive channel plate detector with wedge and strip readout. Their time of flight is measured by a coincidence with the charge state selected projectiles (see Figs. 1 and 3).

In this paper we report on differential double-capture cross sections summed over all final states at 0.25-, 0.5-, and 0.75-MeV impact energy measured by applying COLTRIMS with a scattering-angle resolution of about a factor of 5 better than obtainable by conventional projectile detections [44]. Moreover, at 0.25 MeV we measured the first differential cross sections separated for resonant double capture and double capture to excited states.

II. EXPERIMENT

The typical momenta transferred to the recoil ions in the present collision system are in the range of a few atomic units (a.u.). The momentum distribution of He at room temperature has a width of 4.5 a.u. Thus the experimental key to a measurement of recoil ion momenta is the use of an internally cold and localized gas target provided by a supersonic expansion.

The He gas expands through a 30-μm hole from a reservoir which is mounted on a cryogenic cold head. This allows to cool the He gas to 15 K prior to the supersonic expansion. 10 mm above the nozzle the central part of the gas jet enters the collision chamber through a skimmer of 0.3-mm diameter. This jet is intersected by the collimated ion beam. At

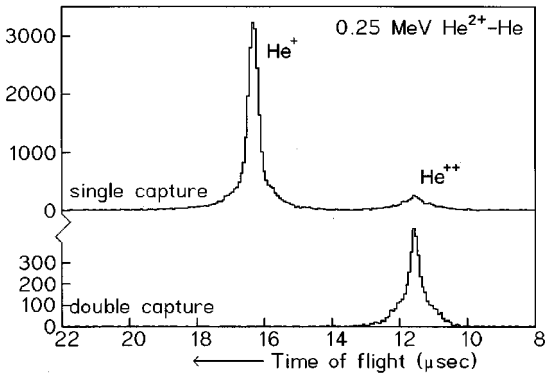

FIG. 3. Time-of-flight distribution of He recoil ions in coincidence with He^+ ejectiles (upper spectrum) and He ejectiles (lower spectrum). The width of the peaks reflects the momentum distribution of the recoil ions in direction of the electric field.

the interaction point, about 25 mm above the skimmer the jet has a diameter of 1 mm. The target gas atoms in the jet have an offset velocity in the jet direction of about 1.4 a.u. The momentum spread around this offset velocity is given by the speed ratio, and is calculated from the parameters of the expansion to be below 0.05 a.u. [46]. In the two directions perpendicular to the jet velocity, the atoms have a momentum spread of about 0.05 a.u. defined by the diameter of the skimmer and its distance to the nozzle. The gas jet leaves the collision chamber through a 10-mm hole into a separately pumped jet dump.

The experiment was performed at the 2-MV van de Graaff accelerator of the Institut für Kernphysik of the Universität Frankfurt. He^+ ions from an ion source are accelerated and then stripped to He^{2+} by a gas stripper and charge

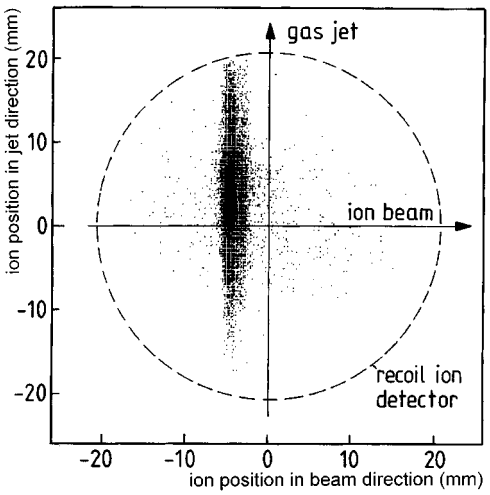

FIG. 4. Recoil ion position distribution on the channel plate detector in Fig. 2 for 0.25-MeV He^{2+} on He collisions. Plotted only are counts which were coincident with a He ejectile and had a time of flight close to the He^{2+} peak (lower spectrum, Fig. 3). The ions are shifted backwards with respect to the gas jet due to their longitudinal momentum from the double-capture reaction, and shifted upwards with respect to the ion beam due to the 1.4-a.u. offset velocity of the gas jet.

state analyzed by a magnet. The He^{2+} beam is collimated by two sets of adjustable slits to a beam-spot size of below 0.5×0.5 mm^2 at the interaction point, and a divergence of below 0.5 mrad. The ion beam is crossed with the supersonic He gas jet. 20 cm upstreams of the intersection point a set of electrostatical deflectors allows one to clean the beam from charge state impurities. 20 cm downstreams of the target a second set of deflectors separates the final projectile charge states. The projectiles which captured one or two electrons are then detected by a two-dimensional position-sensitive channel plate detector with wedge and strip readout. The detector has an active area of 42-mm diameter and a position resolution of 0.2 mm. In Fig. 1 the two-dimensional distribution of the count rate on this detector is shown with the He and He^+ ejectiles well separated.

The recoil ions created at the intersection point are accelerated by a homogeneous electrical field of 0.33 V/cm and a length of 30 mm (see Fig. 2 for the spectrometer). The electric field is perpendicular to the ion beam and the gas jet. The recoil ions exit from the electric-field region into a 60-mm drift tube. Drift and acceleration area are separated by a woven mesh. At the end of the drift tube the ions pass a stack of three grids and are postaccelerated with 2000 V onto another position-sensitive channel plate detector.

The time of flight of the ions in the spectrometer is measured by a coincidence with the charge-exchanged projectiles. Figure 3 shows the time-of-flight distribution of the ions in coincidence with single capture (the right peak of Fig. 1) and double-capture events (the left peak of Fig. 1). From the time of flight one obtains the charge state and the momentum component of the recoil ion in the field direction. The two momentum components perpendicular to the field are calculated from the position on the recoil ion channel plate. Figure 4 shows the distribution of the He^{2+} ions from double-capture collisions on this detector. The momentum resolution in these two directions is restricted by the extension of the interaction volume, and not by the internal momentum spread of the gas jet. In the present experiment a resolution of 0.38-a.u. full width at half maximum (FWHM) for the He^{2+} ions has been achieved. For singly charged ions the resolution of the apparatus is 0.24-a.u. FWHM in the ion-beam direction (see Fig. 5 and Refs. [7,8]).

III. RESULTS AND DISCUSSION

For 0.25-MeV impact energy the longitudinal momentum distribution of the recoil ions integrated over all scattering angles is shown in Fig. 5. From fitting two Gaussians to the spectrum, as shown in the figure, we obtain a fraction of $15.6\pm3\%$ for the capture to all nonautoionizing states to resonant double capture at 0.25 MeV. At 0.5-MeV impact energy we find $16\pm3\%$. This is in excellent agreement with calculations in a four-body classical trajectory Monte Carlo approach by Tökesi and Hock [47], and gives a definite answer to the speculation about the the fraction of excited states included in all previous experimental data which came up in comparing to theories which only accounted for the resonant channel [31,26].

For comparison Fig. 5(b) shows the equivalent spectrum for the single-electron-capture channel from Mergel *et al.* [7]. This spectrum was taken with the same apparatus. Con-

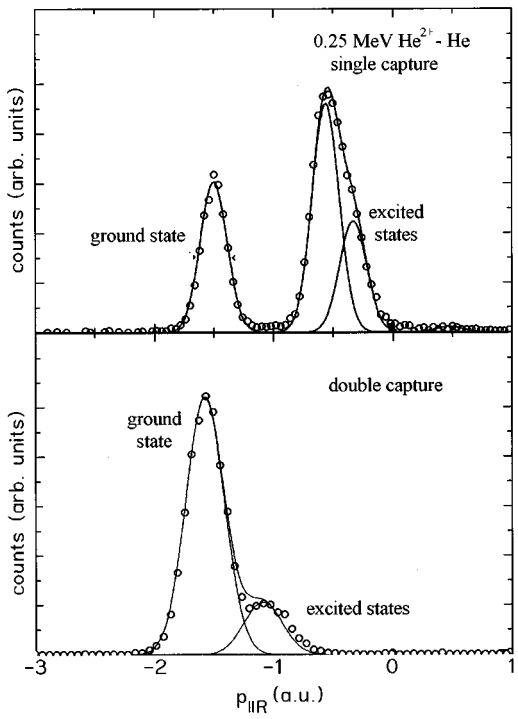

FIG. 5. Momentum distribution of the recoil ions in direction of the ion beam ($p_{\|\mathrm{rec}}$). Upper figure: 0.25-MeV He^{2+} on He single capture (from Ref. [7]). The different peaks relate to different energy changes of the projectile (left peak: ground-state capture with target in the ground state; other peaks: capture to excited states or ground-state capture with target excitation (according to Ref. [12], target excitation is a minor contribution). Lower figure: Same for double-electron capture. Left peak: ground-state capture; right peak: capture to any nonautoionizing excited state. This spectrum is a background corrected projection of Fig. 4 onto the x axis.

trary to double capture, single capture leads most likely to excited states at 0.25-MeV impact energy. This can be explained by considering the binding energies in the initial and final states. For double capture the ground state is resonant, while for single capture the neutral He binding energy is closer to the He^+ L shell than to the K shell.

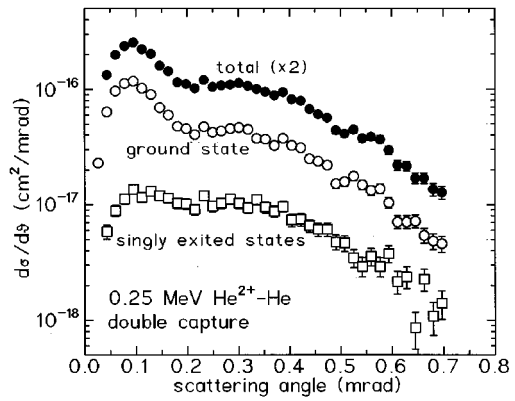

FIG. 6. Scattering angle distribution of double electron capture for 0.25-MeV He^{2+} on He collisions. Full circles: all final states (data multiplied by 2); open circles: ground-state capture; open squares: double capture to nonautoionizing excited states.

Figure 6 shows a distinct maximum for the resonant double capture at a scattering angle of 0.09 mrad. This corresponds to a transverse momentum transfer of only 1 a.u. Such a small momentum can easily be transferred by the electrons changing from the target to the projectile nucleus. It is thus not necessarily due to the internuclear repulsion. For single capture in 0.3 MeV p on He collisions, it has been demonstrated theoretically [48,49] that the by far dominant part of the transverse momentum transfer up to 3 a.u. is mediated by the captured electron. The Thomas mechanism is another example where the transverse momentum is transferred via the electron. The shape of the differential cross section for the resonant channel at small scattering angles should thus reflect the full four-body momentum exchange providing a sensitive test for four-body calculations. At large momentum transfer, which is unlikely to be achieved by two electrons, the scattering angle reflects the internuclear impact parameter. Our finding, that the differential cross section for the double-electron capture to an excited state peaks at much larger scattering angles than the resonant transfer, indicates that smaller impact parameters are necessary to populate these states. For these channels the initial and final states are very different in momentum and energy space. To transfer this momentum and energy from the projectile nucleus to the electrons, close encounters are necessary.

Different types of independent-electron approximations have been used throughout the literature for calculating double-electron capture. Their main differences are the effective binding energies assumed to calculate the first and second steps. The huge experimental difference in the final-state distribution found for single- and double-electron capture, together with the scattering-angle-dependent data, show directly that both processes cannot be understood by the most simple approximation of the same binding energy for both steps for double transfer and single capture. If one aims to describe the double-electron capture within an independent two-step approximation, then modified binding energies for the first and second steps must be assumed. This has already be pointed out by Shingal and Lin [21] and Crothers and co-workers [30–32]. Certainly a full four-body calculation which goes beyond the independent-particle model seems to be the more adequate approach to reproduce the final-state distribution found in this experiment.

Figure 7 shows the double-capture cross section, including all nonautoionizing states differential in projectile scattering angle for 0.25-, 0.5-, and 0.75-MeV impact energy of He^{2+}. The data of Fig. 6 as well as Fig. 7 have been normalized to a total cross section for double capture of 3.17×10^{-17}, 4.73×10^{-18}, and 8.88×10^{-19} cm^2 at 0.25, 0.5, and 0.75 MeV. which are the recommended data from Ref. [50]. The authors gave an error of 20% for these absolute cross sections. The structure in the differential cross section, which is best visible at the lowest energy, may be due to interference between the two elastic-scattering amplitudes. At even lower energy much more pronounced interference patterns have been found [45]. Mergel *et al.* [8] already showed that interferences can be found for He^{2+} on He single capture to the K shell at impact energies up to 0.75 MeV. This is surprising, however, since at 0.75 MeV the velocity of the projectile is already 2.7 a.u., which is two times larger than the electron velocity in the He ground state.

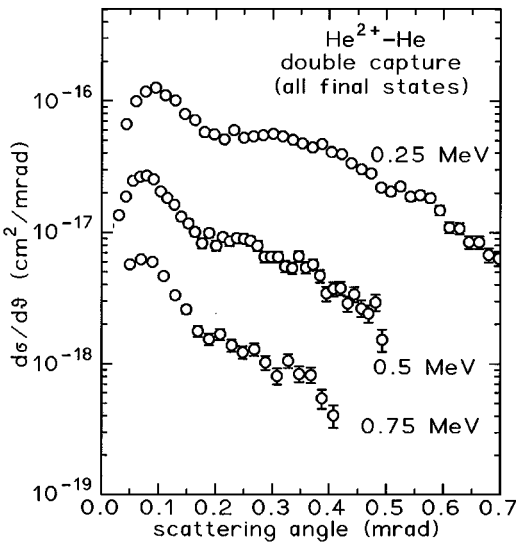

FIG. 7. Scattering angle distribution for 0.25-, 0.5-, and 0.75-MeV He^{2+} on He double-electron capture, summed over all non-autoionizing final projectile states.

At all three impact energies we find the prominent peak at scattering angles below 0.1 mrad. As discussed above, this peak results from the large impact parameter ground-state double capture. The peak maximum moves to smaller scattering angles when going to higher impact energies. Considering the transverse momentum transfer ($p_\perp$) instead of the scattering angle [Eq. (2)], one finds an energy-independent position for the peak maximum within our experimental resolution. At scattering angles above 0.2 mrad we find a steeper decrease of the cross section with increasing impact energy. This reflects mainly the change in Coulomb deflection with energy.

Although our scattering-angle resolution is better than $\pm 10^{-5}$ rad, we do not find any structure from Thomas-type mechanisms. Belkic predicted three maxima in the differential double-capture cross section resulting from different higher-order contributions [39] at high impact energies: at 0.118 and 0.236 mrad, one would expect the contributions due to one- and two-electron Thomas scattering events (for these two contributions, see also Ref. [23]). At 0.136 mrad a third peak is predicted to arise resulting from three successive steps of projectile nucleus-electron, electron-electron, and electron-target nucleus interaction [39]. Since these three mechanisms yield very similar and very small scattering angles, COLTRIMS is the only experimental technique which would allow one to separate them in momentum space. However, higher impact energies than used in the present work seem to be necessary to see these structures clearly.

IV. CONCLUSION

Using COLTRIMS, we determined the first state-selective scattering angle-dependent cross sections for He^{2+} on He double-electron capture. At intermediate energies between 0.25 and 0.75 MeV, we find for all scattering angles that the predominant fraction of the double-capture collisions leads to the ground state of the projectile. Capture to excited states results in larger transverse momentum exchange between projectile than ground-state double capture and target, indicating the necessity of smaller impact parameters for exothermic channels. Due especially to the high resolution in scattering angle, our data provide a profound test ground for the most advanced double-capture theories. Since COLTRIMS enables high-precision scattering-angle measurement without disturbing the ion beam, it is ideally suited for future storage ring experiments: at 5-MeV He impact the current apparatus yields a scattering-angle resolution of better than 0.005 mrad. Together with the high-beam intensity and background-free environment of a storage ring, this opens the unique opportunity to resolve the different types of higher-order Thomas scattering mechanisms [39,23] predicted for double capture at high impact energies. Such experiments are in preparation at CRYRING in Stockholm.

ACKNOWLEDGMENTS

The work was financially supported by DFG and BMFT. The authors appreciate helpful discussions with C. L. Cocke, Dz. Belkic, R. E. Olson, W. Fritsch, H. J. Lüdde, R. Dreizler, W. Wu, and R. Ali.

[1] M. S. Gravielle and J. E. Miraglia, Phys. Rev. A **45**, 2965 (1992).

[2] H. O. Folkerts, R. Hoekstra, L. Meng, R. E. Olson, W. Fritsch, R. Morgenstern, and H. P. Summers, J. Phys. B **26**, L619 (1993).

[3] T. J. M. Zouros, D. Schneider, and N. Stolterfoht, Phys. Rev. A **35**, 1963 (1987).

[4] J. Ullrich, R. Moshammer, R. Dörner, O. Jagutzki, V. Mergel, H. Schmidt-Böcking, and L. Spielberger, J. Phys. B **30**, 2917 (1997).

[5] R. Dörner, J. Ullrich, O. Jagutzki, S. Lencinas, A. Gensmantel, and H. Schmidt-Böcking, in *Electronic and Atomic Collisions, Invited Papers of the ICPEAC XVII*, edited by W. R. MacGillivray, I. E. McCarthy, and M. C. Standage (Hilger, Bristol, 1991), p. 351.

[6] R. Ali, V. Frohne, C. L. Cocke, M. Stöckli, S. Cheng, and M. L. A. Raphaelian, Phys. Rev. Lett. **69**, 2491 (1992).

[7] V. Mergel, R. Dörner, J. Ullrich, O. Jagutzki, S. Lencinas, S. Nüttgens, L. Speilberger, M. Unverzagt, C. L. Cocke, R. E. Olson, M. Schulz, U. Buck, E. Zanger, W. Theisinger, M. Isser, S. Geis, and H. Schmidt-Böcking, Phys. Rev. Lett. **74**, 2200 (1995).

[8] V. Mergel, R. Dörner, J. Ullrich, O. Jagutzki, S. Lencinas, S. Nüttgens, L. Spielberger, M. Unverzagt, C. L. Cocke, R. E. Olson, M. Schulz, U. Buck, and H. Schmidt-Böckiing, Nucl. Instrum. Methods Phys. Res. B **98**, 593 (1995).

[9] A. Cassimi, S. Duponchel, X. Flechard, P. Jardin, P. Sortais, D. Hennecart, and R.E. Olson, Phys. Rev. Lett. **76**, 3679 (1996).

[10] T. Kambara, J. Z. Tang, Y. Awaya, B. D. DePaola, O. Jag-

utzki, Y. Kanai, M. Kimura, T. M. Kojima, V. Mergel, H. W. Schmidt-Böcking, and I. Shimamura, J. Phys. B **28**, 4593 (1995).
[11] R. Moshammer, J. Ullrich, M. Unverzagt, W. Schmidt, P. Jardin, R. E. Olson, R. Mann, R. Dörner, V. Mergel, U. Buck, and H. Schmidt-Böcking, Phys. Rev. Lett. **73**, 3371 (1994).
[12] W. Fritsch, J. Phys. B **27**, 3461 (1994).
[13] M. Kimura, J. Phys. B **21**, L19 (1988).
[14] C. Harel and A. Salin, J. Phys. B **13**, 785 (1980).
[15] K. Gramlich, N. Grün, and W. Scheidt, J. Phys. B **22**, 2567 (1989).
[16] K. R. Sandhya and J. D. Garcia, J. Phys. B **16**, 2837 (1980).
[17] K. J. Schaudt, N. H. Kwong, and J. D. Garcia, Phys. Rev. A **43**, 2294 (1991).
[18] W. Stich, H. J. Lüdde, and R.M. Dreizler, J. Phys. B **18**, 1195 (1985).
[19] C. Chaudhuri, S. Sanyal, and T. K. RaiDastidar, Phys. Rev. A **52**, 1137 (1995).
[20] J. H. McGuire and L. Weaver, Phys. Rev. A **16**, 41 (1977).
[21] R. Shingal and C. D. Lin, J. Phys. B **24**, 251 (1991).
[22] G. Deco and N. Grün, Z. Phys. D **18**, 339 (1991).
[23] A. E. Martinez, R. Gayet, J. Hanssen, and R. D. Rivarola, J. Phys. B **27**, L375 (1994).
[24] R. Gayet, R. D. Rivarola, and A. Salin, J. Phys. B **14**, 2421 (1981).
[25] M. Gosh, C.R. Madal, and S. C. Murkhajee, J. Phys. B **18**, 3797 (1985).
[26] R. Gayet, J. Hanssen, J. Martinez, and R. D. Rivarola, Z. Phys. D **18**, 345 (1991).
[27] T. C. Theisen and J. H. McGuire, Phys. Rev. A **20**, 1406 (1979).
[28] R. E. Olson, J. Phys. B **15**, L163 (1981).
[29] R. E. Olson, A. E. Wetmore, and M. L. McKenzie, J. Phys. B **19**, L629 (1986).
[30] D. S. F. Crothers and R. McCarroll, J. Phys. B **20**, 2835 (1987).
[31] K. M. Dunseath and D. S. F. Crothers, J. Phys. B **24**, 5003 (1991).
[32] N. C. Deb and D. S. F. Crothers, J. Phys. B **23**, L799 (1990).
[33] B. Bhattacharjee, M. Das, N. C. Deb, and S. C. Murkherjee, Phys. Rev. A **54**, 2973 (1996).
[34] Dz. Belkic, Phys. Rev. A **47**, 189 (1993).
[35] Dz. Belkic, J. Phys. B **26**, 497 (1993).
[36] Dz. Belkic and I. Mancev, Phys. Scr. **47**, 18 (1993).
[37] Dz. Belkic and I. Mancev, Phys. Scr. **45**, 35 (1993).
[38] Dz. Belkic, Phys. Rev. A **47**, 189 (1993).
[39] Dz. Belkic, Phys. Rev. A **47**, 3824 (1993).
[40] R. Gayet, J. Hanssen, J. Martinez, and R. B. Rivarola, Nucl. Instrum. Methods Phys. Res. B **86**, 158 (1994).
[41] L. I. Pivovar, X. Tubavaev, and M. T. Novikov, Zh. Éksp. Teor. Fiz. **42**, 1490 (1962) [Sov. Phys. JETP **15**, 1035 (1962)].
[42] R. D. Bois, Phys. Rev. A **36**, 2585 (1987).
[43] N. V. de Castro Faria, F. L. Freire,Jr., and A. G. de Pinho, Phys. Rev. A **37**, 280 (1988).
[44] R. Schuch, E. Justiniano, H. Vogt, G. Deco, and N. Grün, J. Phys. B **24**, L133 (1991).
[45] W. C. Keever and E. Everhart, Phys. Rev. **150**, 43 (1966).
[46] G. Brusdeylins, J. P. Toennies, and R. Vollmer (unpublished).
[47] K. Tökesi and G. Hock, J. Phys. B **29**, L119 (1996).
[48] Dz. Belkic and A. Salin, J. Phys. B **11**, 3908 (1978).
[49] Dz. Belkic and A. Salin, J. Phys. B **11**, 3905 (1978).
[50] C. F. Barnett, in *Atomic Data for Fusion, Collsions of H, H_2, He and Li Atoms with Atoms and Molecules*, edited by I. Alvarez, C. Cisneros, and R. A. Phaneuf (Controlled Fusion Atomic Data Center, Springfield, 1990), Vol. 1, p. A-32.